Analysis of Linear Turbo Equalizer via EXIT Chart

Seok-Jun Lee, Andrew C. Singer, and Naresh R. Shanbhag
Coordinated Science Laboratory, ECE Dept.
University of Illinois at Urbana-Champaign
1308 West Main Street, Urbana, IL 61801
Email: [slee6,acsinger,shanbhag]@uiuc.edu

***Abstract*— In this paper, we propose a method for analysis of linear turbo equalization based on extrinsic information transfer (EXIT) charts. Given channel knowledge and therefore the optimum linear equalizer coefficients, evolution of soft information of the soft-input soft-output (SISO) equalizer can be estimated via computing bit error rates (BER) analytically. Compared to conventional analysis methods, the proposed method predicts the linear turbo equalizer performance without running extensive simulations to obtain the SISO equalizer EXIT charts. Using an empirically generated SISO decoder EXIT chart, convergence analysis can be undertaken. Further, the method provides a bound on the achievable BER for given channels and an estimate of equalizer complexity. These approximate analyses are validated via computer simulations.**

I. Introduction

A wide variety of communication systems encounter intersymbol interference (ISI) in transmission over frequency selective channels. To combat ISI, digital communication receivers are often equipped with an equalizer and use additional forward error correction to remove residual errors. In conventional solutions, equalization and decoding are separate (see Fig 1), which is usually suboptimal in terms of minimizing bit-error rate (BER). After the discovery of turbo codes [1], *turbo equalization* was proposed as a method for joint equalization and decoding, which provides additional gains beyond those obtained from separate equalization and decoding [2]–[7]. The original scheme [2] used a maximum *a posteriori* (MAP) detector with a MAP decoder. However, this scheme often suffers from an enormous computational burden [3]–[6]. To overcome this problem, several low complexity approaches have also been proposed [3]–[6]. Among these low complexity schemes, the linear turbo equalizer based on an interference canceler, introduced by Laot and Glavieux [3], [4], and those based on minimum mean square error (MMSE) criteria (and their low complexity various [5], [6]) have gained great interest because it achieves good performance with reasonable complexity. This achievement motivates additional research into investigation of iterative behavior of linear turbo equalizers.

There has been a fair amount of research on the convergence analysis of iterative schemes [5], [8]–[10]. In [5] and [8], mutual information transfer characteristics of soft-input soft-output (SISO) decoders are proposed to understand convergence behavior and in [9], several measures for tracing convergence are compared for iterative equalizers and decoders. In [10] the evolution of the noise variance is employed to obtain an approximate convergence analysis. However, in all these approaches, the soft information evolution characteristics of SISO equalizers must be obtained numerically through extensive computer simulations. In this paper, the soft information evolution characteristics are estimated by computing the BER analytically, without running simulations. At first, given channel knowledge and a given set of equalizer coefficients, the BER of the linear SISO equalizer at the first iteration and after convergence are derived and mapped onto the EXIT chart. Then, the soft information evolution characteristics are approximated as linear on the EXIT chart [5], [9] and convergence and complexity analyses are undertaken. Further, performance bounds after convergence can be predicted.

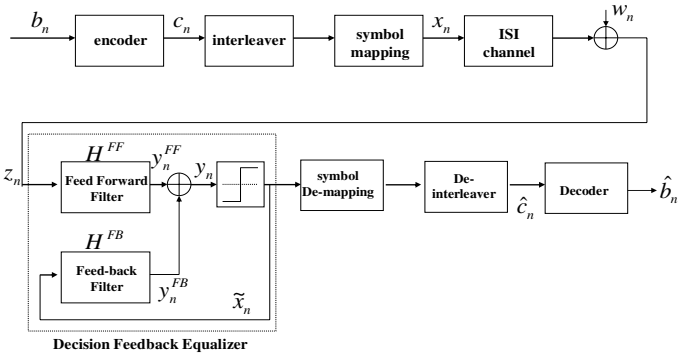

Fig. 1. A conventional communication system, in which the equalization algorithm (shown as a DFE here) and the decoding algorithm operate separately.

The rest of this paper is organized as follows. After a review of linear turbo equalization in the next section, the EXIT chart tool is described briefly in Section III. In Section IV, the BER performance of a linear equalizer is derived and our proposed analysis method is explained. Simulation results and some discussions are provided in Section V, and Section VI concludes this paper.

II. Basics of Linear Turbo Equalizer

This section briefly describes the linear turbo equalization scheme considered [3], [4]. For simplicity, we assume binary phase shift keying (BPSK) modulation, but extension to higher-order modulation is straightforward and is described in greater detail in [4] and [6].

The system to be investigated has a transmitter as described in Fig. 1 with block-based transmission. The binary data b_n is encoded yielding the coded sequence c_n, the interleaver

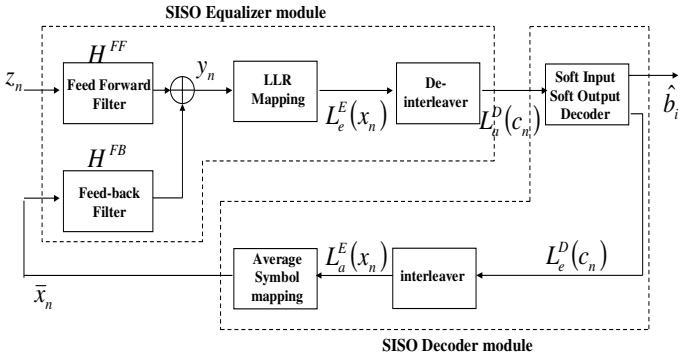

Fig. 2. A linear turbo-equalizer block diagram, in which soft information is exchanged between the equalizer and decoder and the superscript E and D denote equalization and decoding, respectively.

permutes the coded sequence, and then BPSK modulated symbols $x_n \in \{-1, +1\}$ are transmitted over an ISI channel with additive white Gaussian noise (AWGN). The channel output z_n is given by

$$z_n = \sum_{k=-l_1}^{l_2} h_k x_{n-k} + w_n, \tag{1}$$

for a channel response h_k and noise sequence w_n.

Figure 2 depicts the architecture of the linear turbo-equalizer considered in this paper. There are several linear turbo equalization architectures proposed in the literatures [3]–[6], but the interference canceler architecture [3], [4] is employed since it has the minimum hardware complexity. This linear SISO equalizer consists of two operations: symbol estimation and soft-information mapping. The first operation, estimation, is implemented via a linear filter, and the overall architecture is similar to that of the well-known decision-feedback equalizer (DFE) in Fig. 1. However, instead of hard decisions (quantized), soft symbols $\bar{x}_n$ are passed to a feedback filter from the previous iteration of the SISO decoder and the feedback filter removes the residual ISIs after feedforward filter. The logarithm of the likelihood ratio (LLR) mapping block converts each estimated symbol to a log-likelihood $L_e^E(\cdot)$. The LLR of each bit contained in the estimated symbol $\hat{x}_n$ is calculated as

$$L_e^E(x_n) = \ln \frac{Pr(x_n = +1|\hat{x}_n)}{Pr(x_n = -1|\hat{x}_n)}, \tag{2}$$

for BPSK signals.

The equalizer output samples and $L_e^E(\cdot)$ are fed to the SISO decoder, and the decoder updates the extrinsic information on coded bits, c_n, and produces $L_e^D(\cdot)$, the LLR of each coded bit. In turn, $L_e^D(\cdot)$ is passed to a soft output mapping block and then converted to the average symbol value, $\bar{x}_n$. Assuming BPSK, $\bar{x}_n$ is computed as

$$\bar{x}_n = E\{x_n\} = Pr\{x_n = 1\} \cdot 1 + Pr\{x_n = -1\} \cdot -1 \tag{3}$$

$$\bar{x}_n = \frac{\exp(L_a^E(x_n))}{1 + \exp(L_a^E(x_n))} + \frac{-1}{1 + \exp(L_a^E(x_n))}, \tag{4}$$

where $E\{\cdot\}$ denotes a statistical expectation and $L_a^E(x_n)$ is the interleaved version of $L_e^D(c_n)$. This soft information, the averaged symbol, is then fed back to the equalizer block for the next iteration. The details of such a SISO decoder algorithm are described in [11]–[13].

III. The EXIT chart tool

In this section, we describe an analysis tool, called an EXIT chart [8], for convergence analysis of turbo equalizers. The EXIT chart traces the convergence of such iterative algorithms by observing the trajectory of a single parameter. In Ten Brink's approach [8], the parameter is the mutual information I_a and $I_e \in [0, 1]$, between *a priori* values (L_a or L_e) and x_n, which is shown to describe the behavior of SISO algorithms accurately [5], [8]–[9].

As discussed in [5], [8], and [14]–[15], the sequence of output $L_e^E(\cdot)$ and $L_e^D(\cdot)$ values, which are considered *a priori* information updated by SISO equalizers and decoders, are reasonably well approximated as independent and identically distributed with

$$f_L(l|x_n) \triangleq f_L(l|X = x_n) = N(\frac{x_n \sigma_L^2}{2}, \sigma_L^2). \tag{5}$$

Since the conditional probability density functions (pdf) of $L_e^E(\cdot)$ and $L_e^D(\cdot)$ are each assumed to be a function of a single parameter, σ_L, the equalization and decoding blocks can be depicted as a transfer function of $L_a^E(\cdot)$ or $L_a^D(\cdot)$ as in Fig. 3.

The mutual information I_a and $I_e \in [0, 1]$ can be computed by using

$$I_a = \frac{1}{2} \sum_{x \in \{\pm 1\}} \int f_{L_a}(l|x) \log_2 \frac{2 f_{L_a}(l|x)}{f_{L_a}(l|+1) + f_{L_a}(l|-1)} dl$$

$$I_e = \frac{1}{2} \sum_{x \in \{\pm 1\}} \sum_{l} f_{L_e}(l|x) \log_2 \frac{2 f_{L_e}(l|x)}{f_{L_e}(l|+1) + f_{L_e}(l|-1)}. \tag{6}$$

In [5] and [8], $L_a(\cdot)$ is assumed to have $N(\frac{x_n \sigma_{L_a}^2}{2}, \sigma_{L_a}^2)$ distribution, the histogram of output LLRs is observed in

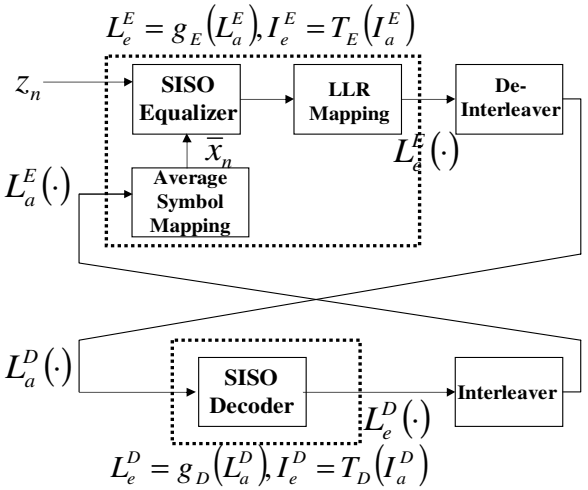

Fig. 3. Modeling L_a, L_e-value update as transfer function.

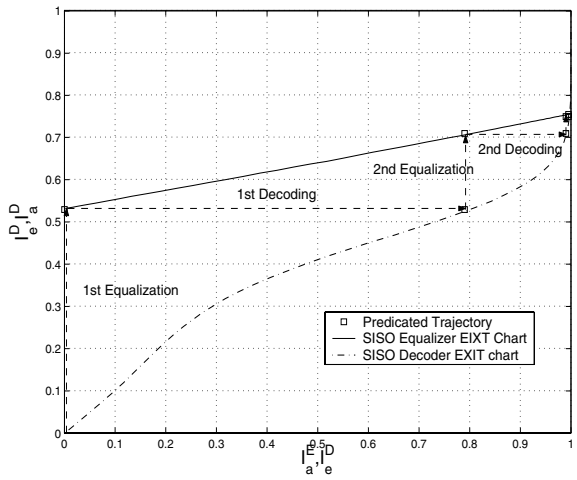

Fig. 4. An example of EXIT chart, in which the mutual information evolutions of SISO equalizer and decoder are obtained experimentally.

extensive simulations in order to estimate the pdf of $L_e(\cdot)$ values of the SISO equalizer and decoder, and then I_a and I_e are computed numerically using (6). Here, $I_a = 0$ and $I_a = 1$, mutual information between the input *a priori* and x_n, imply no and perfect *a priori* information, respectively. When $I_e = 0$ and $I_e = 1$, mutual information between the output *a priori* and x_n, indicate the least and the most reliable soft output information. Thus, if $I_e = 1$ condition is satisfied, the iteration is terminated.

In an EXIT chart tool, the mutual information evolution can be modeled as a transfer function, $I_e^E = T_E(I_a^E = I_e^D)$ or $I_e^D = T_D(I_a^D = I_e^E)$ as shown in Fig. 3 [5]. Then, the iteration process can be visualized as a trace (dashed-arrow line in Fig. 4) between the EXIT charts of the equalizer and decoder by setting $I_e^E \rightarrow I_a^D$ and $I_e^D \rightarrow I_a^E$.

Figure 4 shows an example of EXIT chart analysis. If the equalizer generates soft information ($I_e^E = 0.53$) in the first iteration, then the decoder produces an improved soft output ($I_e^D = 0.78$). This computation can be traced by the dashed-arrow line in the EXIT chart of Fig. 4 and after 3 iterations the $I_e^D = 1$ condition, and corresponding algorithmic convergence, is nearly achieved. Note that, in order to guarantee convergence, a "tunnel" between the two EXIT charts of the equalizer and decoder must appear.

IV. Analysis

In this section, the BER of a linear SISO equalizer is derived. A method for estimating I_e^E of the SISO equalizer from this BER is given, and an approximate analysis method is then described.

A. BER Derivation

Figure 5 describes the model considered in this BER analysis. The overall response of the channel and the receiver equalizer is

$$S_{\hat{x}\hat{x}}(e^{j\omega}) = |\mathbf{H}_{ch}(e^{j\omega})|^2 |\mathbf{H}_{eq}(e^{j\omega})|^2 S_{xx}(e^{j\omega}) + S_{ww}(e^{j\omega})|\mathbf{H}_{eq}(e^{j\omega})|^2. \quad (7)$$

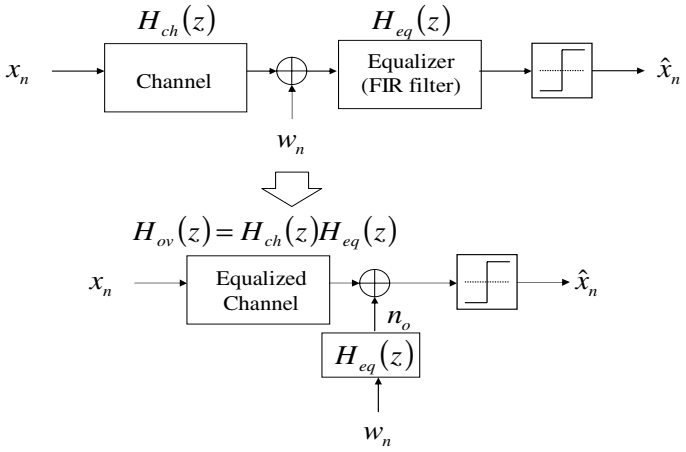

Fig. 5. Conventional communication system with a linear equalizer, where $H_{ov}(z)$ denotes an overall channel response equalized by $H_{eq}(z)$.

The symbol error probability, P_s, is

$$P_s = \sum_{i=1}^{M} \Pr(\hat{S} \neq S_i | S_t = S_i) \cdot \Pr(S_t = S_i), \quad (8)$$

where S_t, $\hat{S}$, and S_i denote the transmitted symbol, estimated symbol, and the ith element from the transmitted alphabet, respectively, and M is the cardinality of the transmitted symbol alphabet. Without loss of generality, it can be assumed that BPSK modulation is used here and that the transmitted symbols are equi-probable. The BER, P_e, can be expressed for a memoryless decision device (a slicer) as

$$\begin{aligned} P_e &= \frac{1}{2}\{\Pr(y_n < 0 | S_t = 1) + \Pr(y_n > 0 | S_t = -1)\} \\ &= \frac{1}{2}\{\Pr(h_{ov}^0 + \sum_{k \neq 0} h_{ov}^k x_k + n_o < 0 | S_t = 1) \\ &\quad + \Pr(-h_{ov}^0 + \sum_{k \neq 0} h_{ov}^k x_k + n_o > 0 | S_t = -1)\}, \end{aligned} \quad (9)$$

where, $\sigma_{n_o}^2 = \sigma_w^2 \sum_k |h_{eq}(k)|^2$ and y_n is the equalizer output. By defining $\mathbf{H}_{ov} \triangleq [h_{ov}^{-M_1}, \cdots h_{ov}^{-1}, h_{ov}^0, h_{ov}^{+1}, \cdots, h_{ov}^{M_2}]^T$, $\mathbf{X}_{-1} \triangleq [-x_{-M_1}, \cdots, -x_{-1}, -1, -x_{+1}, \cdots, -x_{M_2}]^T$, and $\mathbf{X}_{+1} \triangleq [-x_{-M_1}, \cdots, -x_{-1}, +1, -x_{+1}, \cdots, -x_{M_2}]^T$, P_e can be expressed in a compact form as

$$\begin{aligned} P_e = \frac{1}{2}\{ &\sum_{\forall \mathbf{X}_{-1}} \Pr(n_o < \phi) \cdot \Pr(\phi = \mathbf{H}_{ov}^T \cdot \mathbf{X}_{-1}) \\ &+ \sum_{\forall \mathbf{X}_{+1}} \Pr(n_o > \phi) \cdot \Pr(\phi = \mathbf{H}_{ov}^T \cdot \mathbf{X}_{+1})\}. \end{aligned} \quad (10)$$

If transmitted symbols are equi-probable, then

$$\begin{aligned} P_e = \frac{1}{2N}\{ &\sum_{\forall \mathbf{X}_{-1}} \Pr(n_o < \mathbf{H}_{ov}^T \cdot \mathbf{X}_{-1}) \\ &+ \sum_{\forall \mathbf{X}_{+1}} \Pr(n_o > \mathbf{H}_{ov}^T \cdot \mathbf{X}_{+1})\}, \end{aligned} \quad (11)$$

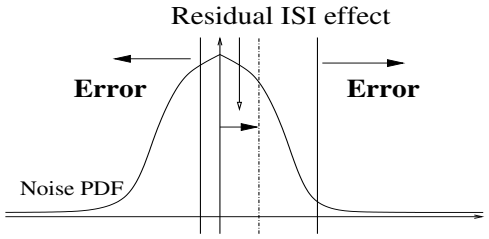

Fig. 6. Decision error region with positive residual ISI.

where, $N = 2^{M_1+M_2}$ is the cardinality of $\mathbf{X}_{-1}$ ($\mathbf{X}_{+1}$). If $\mathbf{X}_0$ is defined as $[-x_{-M_1}, \cdots, -x_{-1}, 0, -x_{+1}, \cdots, -x_{M_2}]$, then

$$\begin{aligned} P_e &= \frac{1}{2N}\{\sum_{\forall \mathbf{X}_0} \Pr(n_o < \mathbf{H}_{ov}^T \cdot \mathbf{X}_0 - h_{ov}^0) \\ &\quad + \sum_{\forall \mathbf{X}_0} \Pr(n_o > \mathbf{H}_{ov}^T \cdot \mathbf{X}_0 + h_{ov}^0)\} \\ &= \frac{1}{2N} \sum_{\forall \mathbf{X}_0} \Pr(|n_o - \mathbf{H}_{ov}^T \cdot \mathbf{X}_0| > h_{ov}^0). \end{aligned} \tag{12}$$

Equation (12) can be interpreted using Fig. 6. The residual ISI caused by adjacent bits in $\mathbf{X}_0$ is $\mathbf{H}_{ov}^T \cdot \mathbf{X}_0$ and it is assumed that n_o has a Gaussian pdf, $f_{n_o} = \frac{1}{\sqrt{2\pi}\sigma} \exp(-\frac{n_o^2}{2\sigma^2})$. Because of residual ISI effects, for each possible $\mathbf{X}_0$ the error region is shifted depending on the sign of residual ISI. Figure 6 shows an example of $\mathbf{H}_{ov}^T \cdot \mathbf{X}_0 > 0$.

Here, we extend the approach to find the BER of the linear turbo equalizer with perfect *a priori* information, in other words after convergence. If y_n is the equalizer output, then we have

$$y_n = \sum_{k=-L_1}^{L_2} h_k^{FF} z_{n-k} - \sum_{k=-K_1}^{K_2} h_k^{FB} \bar{x}_{n-k}, \tag{13}$$

for $L_1 + L_2 + 1$ and $K_1 + K_2 + 1$ taps of feedforward and feedback filters, respectively. In a similar way, we can derive the BER as

$$\begin{aligned} P_e &= \sum_i \Pr(\hat{S} \neq S_t | S_t) \cdot \Pr(S_t) \\ &= \frac{1}{2}\{ \sum_{\forall \mathbf{X}_{-1}, \bar{\mathbf{X}}} \Pr(n_o < \mathbf{H}_{ov}^T \mathbf{X}_{-1} + \mathbf{H}_{FB}^T \bar{\mathbf{X}}) \Pr(\mathbf{X}_{-1}, \bar{\mathbf{X}}) \\ &+ \sum_{\forall \mathbf{X}_{+1}, \bar{\mathbf{X}}} \Pr(n_o < \mathbf{H}_{ov}^T \mathbf{X}_{+1} + \mathbf{H}_{FB}^T \bar{\mathbf{X}}) \Pr(\mathbf{X}_{+1}, \bar{\mathbf{X}})\} \\ &= \frac{1}{2} \sum_{\forall \mathbf{X}_0, \bar{\mathbf{X}}} \Pr(|n_o - \mathbf{H}_{ov}^T \mathbf{X}_0 - \mathbf{H}_{FB}^T \bar{\mathbf{X}}| > h_{ov}^0) \Pr(\mathbf{X}_0, \bar{\mathbf{X}}), \end{aligned} \tag{14}$$

where $\bar{\mathbf{X}}_n$ are the correctly decoded symbols, since perfect *a priori* information is assumed. These coincide with BER calculations for a noncausal DFE with perfect feedback. The analysis results are compared with computer simulations in the next section.

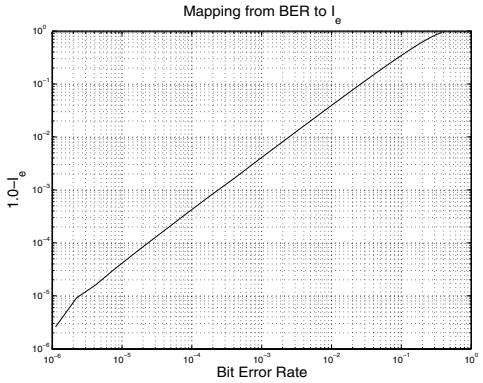

Fig. 7. A mapping function from BER to I_e.

B. Mapping to EXIT chart

In order to find the starting and ending points of the EXIT chart for a SISO equalizer, I_e^E can be estimated based on the analytically computed BER. In [5] and [8], under the Gaussian assumption (5), it is shown that each unique BER corresponds to an unique value of the parameter, I_e, of the output LLRs, $L_e(\cdot)$. For our experiments, we use computer simulations to build a look-up-table mapping a BER to an I_e^E value for the equalizer EXIT chart (see Fig. 7). This approach matches well with simulation results shown in the next Section, and agrees with the results in [5] and [8].

C. Analysis via EXIT charts

Using (12) and (14), the two points, corresponding to I_e^E with no *a priori* information and with perfect *a priori* information respectively, are estimated. Then, since the EXIT chart of linear SISO equalizer appears to be well modeled as linear [5], [9], the equalizer EXIT chart is estimated via two I_e^E values at the points where no *a priori* and perfect *a priori* information are available. This estimated equalizer EXIT chart is projected over the decoder EXIT chart, which is determined experimentally given the encoder polynomial [8]. Hence, given the channel knowledge, linear equalizer coefficients, and the SISO decoder EXIT chart, the performance behavior of a linear turbo equalizer can be investigated without the need to run the usual extensive simulations. By tracing the equalizer and decoder EXIT chart, we can conclude that at least 3 iterations are required to converge to the ideal performance as shown in Fig. 8, where the simulation and analysis results are close to each other but do not match perfectly. Since this EXIT chart analysis is asymptotic (in that the independence assumptions on LLRs hold for an infinite length ideal interleaver [5], [8]) and approximate, we expect such minor mismatch. However, for a finite block length, EXIT charts are still useful in predicting the required minimum number of iterations for convergence and estimating equalization complexity (number of iterations).

V. Experimental results and discussion

In this section, our analysis results are illustrated with computer simulations.

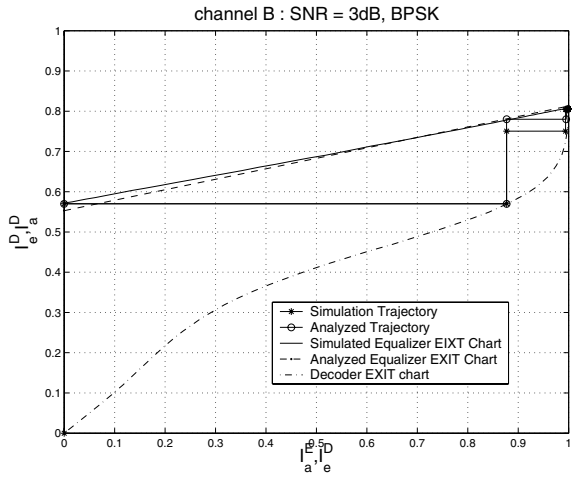

Fig. 8. An example of EXIT chart analysis using the proposed analysis method, where the random interleaver with a length of 4096 is employed.

TABLE I
NUMBER OF TAPS IN SISO EQUALIZATION.

channel	N_{FF}	N_{FB}
A	11	10
B	7	6
C	11	10

A. Simulation setup

We employ a recursive systematic convolutional (RSC) encoder at the transmitter with a generator polynomial $(23, 35)_8$. The coded bit stream is first passed through a random interleaver followed by BPSK modulation. For purposes of comparison, we considered three static channel models (channel **A**, **B**, and **C**),

$$\begin{aligned}
\mathbf{H}_A(z) &= 0.04z^5 - 0.05z^4 + 0.07z^3 - 0.21z^2 - 0.5z \\
&\quad +0.72 + 0.36z^{-1} + 0.21z^{-3} + 0.03z^{-4} \\
&\quad +0.07z^{-5} \\
\mathbf{H}_B(z) &= 0.407z + 0.815 + 0.407z^{-1} \\
\mathbf{H}_C(z) &= 0.227z^2 + 0.46z + 0.688 + 0.46z^{-1} \\
&\quad +0.227z^{-2},
\end{aligned}$$

where $\mathbf{H}_A(z)$ is a good channel (no spectral null), $\mathbf{H}_B(z)$ has medium ISI (spectral null near $\omega = \pi$, and $\mathbf{H}_C(z)$ has severe ISI [16] (strong spectral null near $\omega = 0.6\pi$). We use random interleavers and a MMSE algorithm is used to determine linear equalizer coefficients assuming the perfect channel knowledge at a receiver. The number of taps used in the feedforward path and the feedback path are summarized in Table I. A sliding window Log-MAP decoder [13] is employed and 10 iterations are carried out.

B. Summary of results

Computer simulations are carried out to validate our analysis method and the results are summarized in Table II, where it is clear that our BER analysis results match well simulation results and our I_e values obtained from this BER analysis also match well within an error range of 4.5%. In Table II, analysis results with $I_a^E = 0$ and $I_a^E = 1$ correspond to BER and I_e^E after the first iteration and after convergence respectively. With this approach, the required number of iterations for each channel is summarized in Tables III–V and compared with simulation results. For $\mathbf{H}_A(z)$, the analysis is equal to simulation when using 4K-bit interleaver. However, for $\mathbf{H}_B(z)$ and $\mathbf{H}_C(z)$, the analysis is closer when a larger interleaver (64K-bit interleaver) is employed. Larger interleavers better decorrelate error events introduced by the equalizer between neighboring symbols thereby satisfying the independence assumption on LLRs more closely [5], [8]. It is noticed that our analysis, in which an infinite length interleaver is assumed, provides a good estimate of the required number of iterations.

Further, the slope of the estimated equalizer EXIT chart provides a measure of required complexity (the number of iterations needed for convergence). If the slope is steep ($\mathbf{H}_B(z)$ and $\mathbf{H}_C(z)$), more iterations are required and BER performance improves with iteration as shown in Table II. This means that the output *a priori* information, $L_e^E(\cdot)$, becomes more reliable as the input *a priori* information, $L_a^E(\cdot)$, becomes more reliable. However, when the slope is less steep ($\mathbf{H}_A(z)$), more reliable feedback information from the SISO decoder makes little difference in soft outputs. Hence, after a few iterations, BER improvement ceases as shown in Table II.

By observing the starting point of the equalizer EXIT chart, it can be determined whether further iterations will improve BER or not. If I_e after the first iteration is large (≥ 0.6), further iterations will not improve BER much and hence, a small number of iterations are required for convergence. On the other hand, in the scenario where I_e after the first iteration is small (≤ 0.5), BER improvements are noticeable and more iterations are expected to be carried out so that the desired performance is achieved as shown Table II.

VI. CONCLUDING REMARKS

We proposed a linear turbo equalizer analysis method, where the SISO equalizer EXIT chart is estimated via computing BER analytically given the channel knowledge and the linear equalizer coefficients. Therefore, without the need of extensive simulations, the required number of iterations for convergence, the achievable BER, and a measure of equalization complexity are predicted via EXIT charts. Computer simulations support our analysis results. The work presented in this paper will be of use in finding the required number of iterations and the achievable performance of linear turbo equalizers given a linear SISO equalizer algorithm.

ACKNOWLEDGMENT

This material is based upon work supported by the National Science Foundation under Grant CCR 99-79381, CCR-0092598, and ITR 00-85929.

TABLE II

COMPARISON BETWEEN SIMULATION AND ANALYSIS.

	Bit error rate(BER)						Mutual information (I_e)			
Channel $\mathbf{A}$	Simulation				Analysis		Simulation		Analysis	
SNR	1st	2nd	3rd	10th	$I_a^E=0$	$I_a^E=1$	1st	10th	$I_a^E=0$	$I_a^E=1$
1 dB	0.0795	0.0668	0.0668	0.0668	0.0787	0.0658	0.718	0.759	0.72	0.767
2 dB	0.0599	0.0481	0.0481	0.0481	0.0591	0.0473	0.782	0.822	0.785	0.828
3 dB	0.0433	0.0329	0.0329	0.0329	0.0424	0.0322	0.838	0.874	0.842	0.872
4 dB	0.0296	0.0212	0.0212	0.0212	0.0288	0.0205	0.886	0.916	0.893	0.922
Channel $\mathbf{B}$	Simulation				Analysis		Simulation		Analysis	
SNR	1st	2nd	3rd	10th	$I_a^E=0$	$I_a^E=1$	1st	10th	$I_a^E=0$	$I_a^E=1$
1 dB	0.1612	0.1243	0.0966	0.0871	0.161	0.0856	0.490	0.693	0.485	0.701
2 dB	0.1467	0.0939	0.0709	0.0683	0.1464	0.0679	0.531	0.754	0.524	0.758
3 dB	0.1330	0.0678	0.0531	0.0526	0.1326	0.0523	0.57	0.806	0.552	0.812
4 dB	0.1201	0.0476	0.0395	0.0395	0.1197	0.0392	0.607	0.851	0.592	0.851
Channel $\mathbf{C}$	Simulation				Analysis		Simulation		Analysis	
SNR	1st	2nd	3rd	10th	$I_a^E=0$	$I_a^E=1$	1st	10th	$I_a^E=0$	$I_a^E=1$
6 dB	0.1791	0.1549	0.1102	0.0555	0.1791	0.0550	0.451	0.796	0.43	0.803
7 dB	0.1689	0.1291	0.0755	0.0484	0.1692	0.0483	0.476	0.821	0.459	0.820
8 dB	0.1586	0.1039	0.0515	0.04239	0.1587	0.0422	0.502	0.842	0.485	0.842
9 dB	0.1482	0.0809	0.0390	0.0368	0.1483	0.0366	0.528	0.862	0.513	0.866

TABLE III

THE NUMBER OF ITERATIONS FOR CONVERGENCE (CHANNEL $\mathbf{A}$).

E_b/N_o	4K interleaver	Analysis
1 dB	2	2
2 dB	2	2
3 dB	2	2
4 dB	2	2

TABLE IV

THE NUMBER OF ITERATIONS FOR CONVERGENCE (CHANNEL $\mathbf{B}$).

E_b/N_o	4K interleaver	64K interleaver	Analysis
1 dB	6	5	4
2 dB	4	4	4
3 dB	4	3	3
4 dB	3	3	3

TABLE V

THE NUMBER OF ITERATIONS FOR CONVERGENCE (CHANNEL $\mathbf{C}$).

E_b/N_o	4K interleaver	64K interleaver	Analysis
6 dB	9	7	5
7 dB	8	5	4
8 dB	7	5	4
9 dB	5	4	3

REFERENCES

[1] C. Berrou, A. Glavieux, and P. Thitimajshima, "Near shannon limit error-correcting coding and decoding: Turbo codes," in *Proc. of IEEE Int. Conf. on Comm., Geneva*, May 1993, pp. 1064–1070.

[2] C. Douillard, M. Jezequel, C. Berrou, A. Picart, P. Didier, and A. Glavieux, "Iterative correction of intersymbol interference: Turbo-equalization," *European Transactions on Telecommunications*, vol. 6, pp. 507–511, September-October 1995.

[3] A. Glavieux, C. Laot, and J. Labat, "Turbo equalization over a frequency selective channel," in *Proc. of Int. Symp. on Turbo Codes & Related topics,* September 1997, pp. 96–102.

[4] C. Laot, A. Glavieux, and J. Labat, "Turbo Equalization: Adaptive Equalization and Channel Decoding Jointly Optimized," *IEEE Journal of Selected Areas in Comm.,* vol. 19, pp. 1744–1752, September 2001.

[5] M. Tüchler, R. Koetter, and A. Singer, "Turbo-equalization: principles and new results," *IEEE Trans. on Comm.,* vol. 50, no. 5, pp. 754–767, May 2002.

[6] M. Tüchler, A. Singer, and R. Koetter, "Minimum Mean Squared Error Equalization Using A-Priori Information," *IEEE Trans. on Signal Processing*, vol. 50, pp. 673–683, Mar. 2002.

[7] Z. Wu and J. M. Cioffi, "Turbo decision aided equalization for magnetic recording channels," in *Proc. of Global Telecommunication Conference'99,* 1999, pp. 733–738.

[8] S. ten Brink, "Convergence behavior of iteratively decoded parallel concatenated codes," *IEEE Trans. on Comm.,* vol. 49, pp. 1727–1737, October 1999.

[9] M. Tüchler, S. ten Brink, and J. Hagenauer, "Measures for Tracing Convergence of Iterative Decoding Algorithms," in *Proc. ITG,* Berlin, Germany, Jan. 2002.

[10] A. Roumy, A. J. Grant, I. Fijalkow, P. D. Alexander, and D. Pirez, "Turbo-Equalization : Convergence Analysis," in *Proc. of ICASSP,* no. 4, 2001, pp. 2645–2648.

[11] P. Robertson, E. Villebrun, and P. Hoeher, "A comparison of optimal and sub-optimal MAP decoding algorithms operating in the log domain," in *Proc. of IEEE Int. Conf. on Comm.(ICC),* 1995, pp. 1009-1013.

[12] J. Hagenauer and P. Hoeher, "A Viterbi algorithm with soft-decision outputs and its application," in *Proc. of IEEE Global Telecomm. Conf. '89,* vol. 47, no. 1, 1989, pp. 1680–1686.

[13] A. J. Viterbi, "An Intuitive Justification and a Simplified Implementation of the MAP Decoder for Convolutional Codes," *IEEE Journal on Selected Areas in Communications*, vol. 16, no. 2, pp. 260–264, Feb. 1998.

[14] H. E. Gamal and A. R. Hammons, "Analyzing the Turbo Decoder Using the Gaussian Approximation," *IEEE Trans. on Information Theory*, vol. 47, pp. 671–686, Feb. 2001.

[15] D. Divsalar, S. Dolinar, and F. Pollarar, "Iterative turbo decoder analysis based on density evolution," *IEEE Journal on Selected Areas in Communications*, vol. 19, pp. 891–907, May 2001.

[16] J. G. Proakis, *Digital Communications*, 3rd ed. McGRAW-HILL, 1995.